Neuronal Calcium Sensor-1 and Phosphatidylinositol 4-Kinase β Stimulate Extracellular Signal-regulated Kinase 1/2 Signaling by Accelerating Recycling through the Endocytic Recycling Compartment⟨V⟩

Yaara Kapp-Barnea,*† Lihi Ninio-Many,*† Koret Hirschberg,‡ Mitsunori Fukuda,§ Andreas Jeromin,‖ and Ronit Sagi-Eisenberg*

Departments of *Cell and Developmental Biology and ‡Pathology, Sackler School of Medicine, Tel Aviv University, Tel Aviv 69978, Israel; §Department of Developmental Biology and Neurosciences, Tohoku University, Aobayama, Aoba-ku, Sendai, Miyagi 980-8578, Japan; and ‖Center for Learning and Memory, University of Texas at Austin, Austin, TX 78712

We demonstrate that recycling through the endocytic recycling compartment (ERC) is an essential step in FcεRI-induced activation of extracellular signal-regulated kinase (ERK)1/2. We show that ERK1/2 acquires perinuclear localization and colocalizes with Rab 11 and internalized transferrin in FcεRI-activated cells. Moreover, a close correlation exists between the amount of ERC-localized ERK1/2 and the amount of phospho-ERK1/2 that resides in the nucleus. We further show that by activating phosphatidylinositol 4-kinase β (PI4Kβ) and increasing the cellular level of phosphatidylinositol(4) phosphate, neuronal calcium sensor-1 (NCS-1), a calmodulin-related protein, stimulates recycling and thereby enhances FcεRI-triggered activation and nuclear translocation of ERK1/2. Conversely, NCS-1 short hairpin RNA, a kinase dead (KD) mutant of PI4Kβ (KD-PI4Kβ), the pleckstrin homology (PH) domain of FAPP1 as well as RNA interference of synaptotagmin IX or monensin, which inhibit export from the ERC, abrogate FcεRI-induced activation of ERK1/2. Consistently, NCS-1 also enhances, whereas both KD-PI4Kβ and FAPP1-PH domain inhibit, FcεRI-induced release of arachidonic acid/metabolites, a downstream target of ERK1/2 in mast cells. Together, our results demonstrate a novel role for NCS-1 and PI4Kβ in regulating ERK1/2 signaling and inflammatory reactions in mast cells. Our results further identify the ERC as a crucial determinant in controlling ERK1/2 signaling.

INTRODUCTION

Neuronal calcium sensor-1 (NCS-1), a 22-kDa calmodulin-related protein, belongs to the superfamily of EF-hand Ca^{2+}-binding proteins (Burgoyne and Weiss, 2001; Chen *et al.*, 2002). NCS-1 is conserved through evolution with orthologues identified in yeast, *Xenopus*, *Caenorhabditis elegans*, *Drosophila* (first identified and termed frequenin), and avian and mammalian cells (Braunewell and Gundelfinger, 1999; Hendricks *et al.*, 1999; Jeromin *et al.*, 1999; Burgoyne and Weiss, 2001; Chen *et al.*, 2002). In mammalians, NCS-1 is mainly, but not solely, expressed in neurons and neuroendocrine cells where it functions to modulate synaptic trans-mission as well as synaptic plasticity (McFerran *et al.*, 1998; Chen *et al.*, 2002; Sippy *et al.*, 2003). Additionally, NCS-1 stimulates the activity of phosphatidylinositol 4-kinase β (PI4Kβ) (Hendricks *et al.*, 1999; Zhao *et al.*, 2001; Kapp-Barnea *et al.*, 2003; Rajebhosale *et al.*, 2003; Haynes *et al.*, 2005) and thereby modulates phosphatidylinositol-dependent signaling (Kapp-Barnea *et al.*, 2003; Rajebhosale *et al.*, 2003). Previously, we have shown that NCS-1 regulates FcεRI-triggered exocytosis in mast cells by stimulating PI(4)P production and increasing the pool of phosphatidylinositol 4,5-bisphosphate [PI(4,5)P$_2$] that is required for lipid-derived second messenger generation by the receptor-activated phospholipase C (PLC) (Kapp-Barnea *et al.*, 2003). However, the role of phosphoinositides is not restricted to second messenger generation. These lipids have emerged as key players in the control of a variety of cellular functions. By binding proteins that contain specific phosphoinositide binding domains, such as pleckstrin homology (PH), FYVE, ENTH/ANTH, and PX or basic stretches such as the C2 domains, phosphoinositides facilitate their membrane localization or allosterically modulate their function (De Camilli *et al.*, 1996; Katan and Allen, 1999; Cockcroft and De Matteis, 2001; Hurley and Meyer, 2001; Itoh and Takenawa, 2002; De Matteis *et al.*, 2002; Birkeland and Stenmark, 2004; Roth, 2004). Moreover, because unique phosphoinositides are found at distinct sites on intracellular membranes, phosphoinositides also contribute to the spatial segregation of

proteins, which contain the appropriate modules. As such, phosphoinositides regulate both trafficking and signaling networks and in particular may affect signaling events that are tightly coupled with protein trafficking. Therefore, we postulated that by modulating the cellular level of phosphoinositides, NCS-1 is most likely to influence a large array of traffic and signaling events.

The mitogen-activated protein kinases (MAPKs) extracellular signal-regulated kinase (ERK)1/2 mediate multiple cellular processes, including growth, survival, differentiation, and inflammatory reactions (Seger and Krebs, 1995; Zhang *et al.*, 1997; Pouyssegur *et al.*, 2002). Previous studies have established that activation of ERK1/2 requires endosomal trafficking (Di Fiore and De Camilli, 2001; Kholodenko, 2002; Miaczynska *et al.*, 2004; Lunin *et al.*, 2004). Because endosomal trafficking is critically regulated by phosphoinositides (Gruenberg, 2003; Itoh and Takenawa, 1993), we set out to investigate whether NCS-1 and its downstream effector PI4Kβ may regulate endocytosis and ERK activation. Here, we demonstrate that NCS-1 promotes activation and nuclear association of ERK1/2. We show that by increasing the cellular level of PI(4)P, NCS-1 stimulates recycling through the endocytic recycling compartment (ERC), and this process is tightly linked with ERK1/2 activation.

MATERIALS AND METHODS

Materials

The protease inhibitor cocktail Complete was obtained from Roche Diagnostics (Indianapolis, IN). Dinitrophenyl (DNP)$_{22}$-conjugated human albumin, monensin, holotransferrin, deferoxamin-mesylate, and horseradish peroxidase (HRP)-conjugated streptavidin were from Sigma-Aldrich (St. Louis, MO). Biotin, Alexa-488, and Texas Red (TR)-conjugated transferrin (Tfn) were obtained from Invitrogen (Carlsbad, CA). [^{3}H]Arachidonic acid (AA) (81.70 Ci/mmol) was obtained from PerkinElmer Life and Analytical Sciences (Boston, MA).

DNA Constructs

Green fluorescent protein (GFP)-Rab 11 cDNA was a generous gift from Dr. Marino Zerial (Max-Planck Institute of Molecular Cell Biology and Genetics, Dresden, Germany). GFP-FAPPI-PH cDNA was a generous gift from Dr. Tamas Balla (Endocrinology and Reproduction Research Branch, National Institute of Child Health and Human Development; National Institutes of Health, Bethesda, MD). Synaptotagmin (Syt) IX short hairpin (sh)RNA (Fukuda, 2004) and NCS-1-yellow fluorescent protein (YFP) (Zhao *et al.*, 2001) were described previously. NCS-1 shRNA was targeted against the rat and human sequence GGCTTCCAGAAGATCTACA. The target sequence as well as a control mismatched sequence was subcloned into the pStrike U1 vector (Promega, Madison, WI) coexpressing YFP.

Antibodies

Monoclonal anti-active ERK1/2 and polyclonal anti-total ERK1/2 antibodies were purchased from Sigma-Aldrich. Polyclonal anti-phospho-Akt was purchased from Cell Signaling Technology (Beverly, MA). Peroxidase-conjugated Affinipure goat anti-mouse and goat anti-rabbit IgGs and the Cy3-conjugated goat anti-mouse IgGs were from Jackson ImmunoResearch Laboratories (West Grove, PA). Monoclonal DNP-specific IgE (SPE-7) was from Sigma-Aldrich. Polyclonal antibodies against NCS-1 were raised in rabbits.

Cell Culture

Mock-transfected rat basophilic leukemia (RBL) cells and RBL cells stably transfected with full-length cDNAs encoding NCS-1 or the kinase dead (KD) mutant of PI4Kβ(KD-PI4KβD656A) were described previously (Kapp-Barnea *et al.*, 2003). The cells were maintained as adherent cultures in DMEM supplemented with 10% fetal calf serum in a humidified atmosphere of 5% CO$_2$ at 37°C.

Transient Transfection

Cells were transiently transfected as described previously (Grimberg *et al.*, 2003; Haberman *et al.*, 2003). Briefly, 8 × 10^6 cells were electroporated (300 V [0.3] 1500 μF) in the presence of 40 μg of the desired DNA and immediately replated in tissue culture dishes containing growth medium (supplemented DMEM).
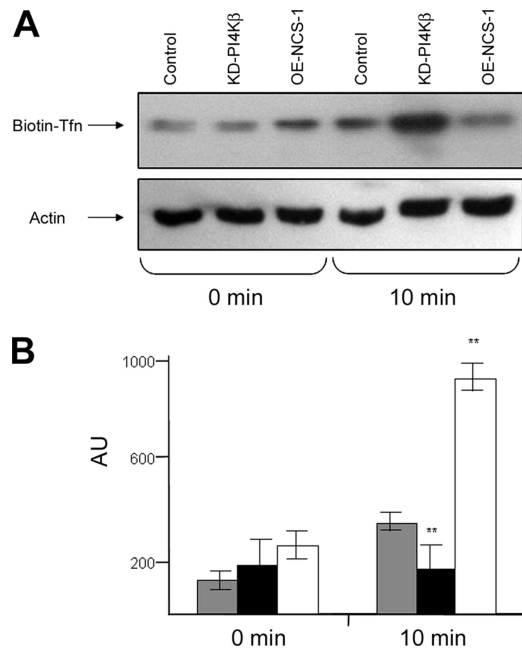
Figure 1. Effect of NCS-1 and KD-PI4Kβ on Tfn endocytosis. Control (mock-transfected), OE-NCS-1 or KD-PI4Kβ cells were serum starved for 1 h and incubated with 20 μg/ml biotin-Tfn for 1 h at 4°C. Unbound biotin-Tfn was removed by washing with ice-cold PBS, and the cells delivered to 37°C (time 0) for 10 min to allow endocytosis. At the end of incubation, cells were placed on ice, and the amount of intracellular biotin-Tfn was determined by subjecting cell lysates to SDS-PAGE, immunoblotting, and probing with HRP-conjugated streptavidin. (A) Blots were visualized by enhanced chemiluminescence (A). The cellular level of actin was determined to judge for equal loading. Blots of three similar experiments were quantified by densitometry and analyzed using one-tailed Mann–Whitney *t* test. The average ± SEM is presented. Shaded columns, control cells; filled columns, OE-NCS-1 cells; and open columns, KD-PI4Kβ cells; **p < 0.01 (B).

Western Blot Analysis

Samples of cell extracts (normalized according to protein content or cell number) were separated by SDS-PAGE using 10% polyacrylamide gels and electrophoretically transferred to nitrocellulose membranes. Blots were blocked for 3 h in Tris-buffered saline/Tween 20 (10 mM Tris-HCl, pH 8.0, 150 mM NaCl, and 0.05% Tween 20) containing 5% skim-milk or 2% bovine serum albumin (BSA) followed by overnight incubation at 4°C with the desired primary antibodies. Blots were washed three times and incubated for 1 h at room temperature with HRP-conjugated secondary antibodies. Immunoreactive bands were visualized by the enhanced chemiluminescence method according to standard procedures.

Stimulation of RBL Cells

RBL cells were plated in 24-well plates (2.5 × 10^5 cells/well) and incubated overnight in a humidified incubator at 37°C with a monoclonal DNP-specific IgE antibody (25 ng/ml). Cells were then washed three times in Tyrode buffer (10 mM HEPES, pH 7.4, 130 mM NaCl, 5 mM KCl, 1.4 mM CaCl$_2$, 1 mM MgCl$_2$, 5.6 mM glucose, and 0.1% BSA) and stimulated at 37°C with DNP-human serum albumin (HAS) (antigen; Ag) (50 ng/ml) for the desired periods.

Determination of ERK1/2 Activation

Cell extracts, derived from activated cells, were prepared by the addition of lysis buffer A (150 mM sucrose, 80 mM β-glycerophosphate, 2 mM EDTA, 2 mM EGTA, 2 mM NaVO$_3$, 10 mM sodium pyrophosphate [NaPPi], and 1% Triton X-100) and resolved by SDS-10% PAGE under reducing conditions. Gels were transferred to nitrocellulose membranes and probed overnight at 4°C with monoclonal antibodies directed against the active phosphorylated form of p42/p44 ERK1/2 (1/20,000 dilution).

Immunofluorescence Microscopy

RBL cells (2.5 × 10^5 cells/ml) were grown on 12-mm round glass coverslips. After incubation for 18 h at 37°C, the medium was aspirated, and the adherent
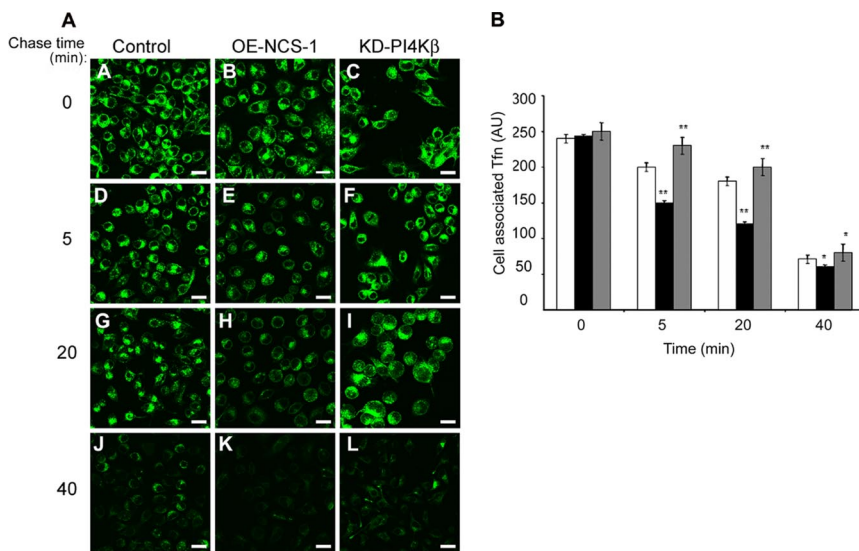
A

B

Figure 2. Effect of NCS-1 and KD-PI4Kβ on Tfn recycling. Control (mock-transfected), OE-NCS-1, or KD-PI4Kβ cells were grown on glass coverslips, serum starved for 1 h, and incubated with 50 μg/ml Alexa-488-Tfn for 1 h at 37°C. Cells were subsequently placed on ice (A–C) or washed and chased with unlabeled 100 μg/ml Tfn in the presence of 100 μM defroxamine mesylate for the indicated times (D–L). Cells were processed and visualized by laser confocal microscopy. Bar, 20 μm (A). To compare the rate of recycling from the ERC, the fluorescence intensity for each cell type at time 0 was normalized, and the fluorescence of 30–80 cells was measured for each time point. The average fluorescence per cell was calculated and is presented as arbitrary units (AU). Open columns, control cells; filled columns, OE-NCS-1 cells; and shaded columns, KD-PI4Kβ cells (B).

cells were washed three times with cold phosphate-buffered saline (PBS). Cells were subsequently fixed for 30 min in 3% paraformaldehyde and permeabilized for additional 30 min by a permeabilization solution (0.1% Triton, 5% fetal calf serum [FCS], and 2% BSA in PBS). To stain the active ERK1/2, cells were activated as described above, fixed and parmeabilized in lysis buffer A (150 mM sucrose, 80 mM β-glycerophosphate, 2 mM EDTA, 2 mM EGTA, 2 mM NaVO₃, 10 mM NaPPi, 1% Triton X-100, 5% FCS, and 2% BSA). For localization of total or active ERK1/2, cells were treated with 100 μg/ml digitonin for 5 min before fixation and permeabilization. Cells were subsequently incubated for 1 h at room temperature with the primary antibodies, washed three times, and incubated for 1 h with the appropriate secondary antibody. Coverslips were subsequently washed five times and mounted with Gel Mount mounting medium (Biomeda, Foster City, CA). Samples were analyzed using a Zeiss laser confocal microscope (Carl Zeiss, Oberkochen, Germany).

Determination of AA/Metabolites Release

Control (mock-transfected), NCS-1–overexpressing (OE-NCS-1) or KD-PI4Kβ–expressing RBL cells were seeded in 24-well plates at 2.5×10^5 cells/well and incubated overnight with monoclonal DNP-specific IgE antibody in the presence of 0.4 μCi/ml [³H]AA at 37°C. The cells were subsequently washed three times in Tyrode's buffer, and triggered for the desired times. Reactions were terminated by placing the dishes at 4°C. Supernatants were collected and used to determine the amount of radiolabeled AA/metabolites released by liquid scintillation.

Quantitative Assay of Tfn Internalization

Tfn internalization was monitored as described previously (Grimberg *et al.*, 2003). Briefly, OE-NCS-1– or KD-PI4Kβ–expressing RBL cells (2.5×10^5) were

serum starved for 1 h at 37°C in DMEM supplemented with 0.2% BSA and 50 mM HEPES, pH 7.4, followed by 1-h incubation at 4°C with 20 μg/ml biotin-conjugated Tfn to allow binding. Unbound Tfn was removed by washing with ice-cold PBS. To allow endocytosis the cells were transferred to 37°C for the desired times. The reaction was stopped by placing the cells on ice. Cells were subsequently processed for Western blot analysis using HRP-conjugated streptavidin.

Tfn Recycling

Recycling was measured as described previously (Grimberg *et al.*, 2003; Haberman *et al.*, 2003). Briefly, OE-NCS-1– or KD-PI4Kβ–expressing RBL cells (2.5×10^5 cells/ml) were grown on 12-mm round glass coverslips, serum starved for 1 h in DMEM supplemented with 0.2% BSA and 50 mM HEPES, pH 7.4, followed by incubation with Alexa-488– or TR-conjugated Tfn (50 μg/ml) for 1 h at 37°C. Cells were washed twice in PBS, and unlabeled 100 μg/ml Tfn and 100 μM deferoxamine mesylate were added. At selected times, incubations were stopped by placing the dishes on ice, and cells were processed for immunofluorescence as described above.

Tfn Recycling by Living Cells

OE-NCS-1– or KD-PI4Kβ–expressing RBL cells (2.5×10^5 cells/ml), grown in Lab-Tek chambered coverglass (Nagle Nunc International, Rochester, NY), were serum starved for 1 h in DMEM supplemented with 0.2% BSA and 50 mM HEPES, pH 7.4, followed by incubation with 50 μg/ml Alexa-488-Tfn for 1 h at 37°C. Cells were washed twice in PBS, and unlabeled 100 μg/ml Tfn and 100 μM deferoxamine mesylate were added. Cells were monitored at 37°C, every 45 s for 1 h, by a Zeiss laser confocal microscope (Carl Zeiss). Images were analyzed using the Zeiss LSM software.
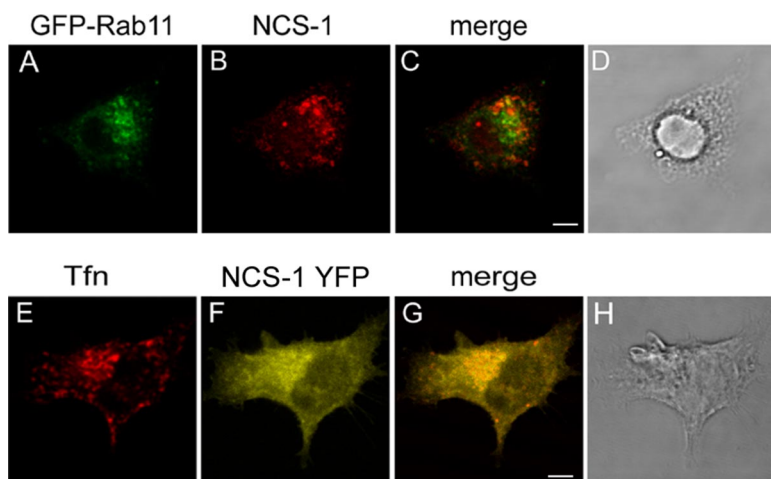

Figure 3. Subcellular localization of NCS-1. OE-NCS-1 cells, transiently transfected with GFP-Rab 11 cDNA (A–D) or RBL cells transiently transfected with NCS-1-YFP cDNA (E–H) were grown on glass coverslips for 24 h. Cells were subsequently either labeled with rabbit polyclonal anti NCS-1 antibodies followed by Cy3-conjugated anti rabbit IgG (A–C) or loaded with TR-conjugated Tfn (E–G). Cells were visualized by laser confocal microscopy. Bar, 4 μm.
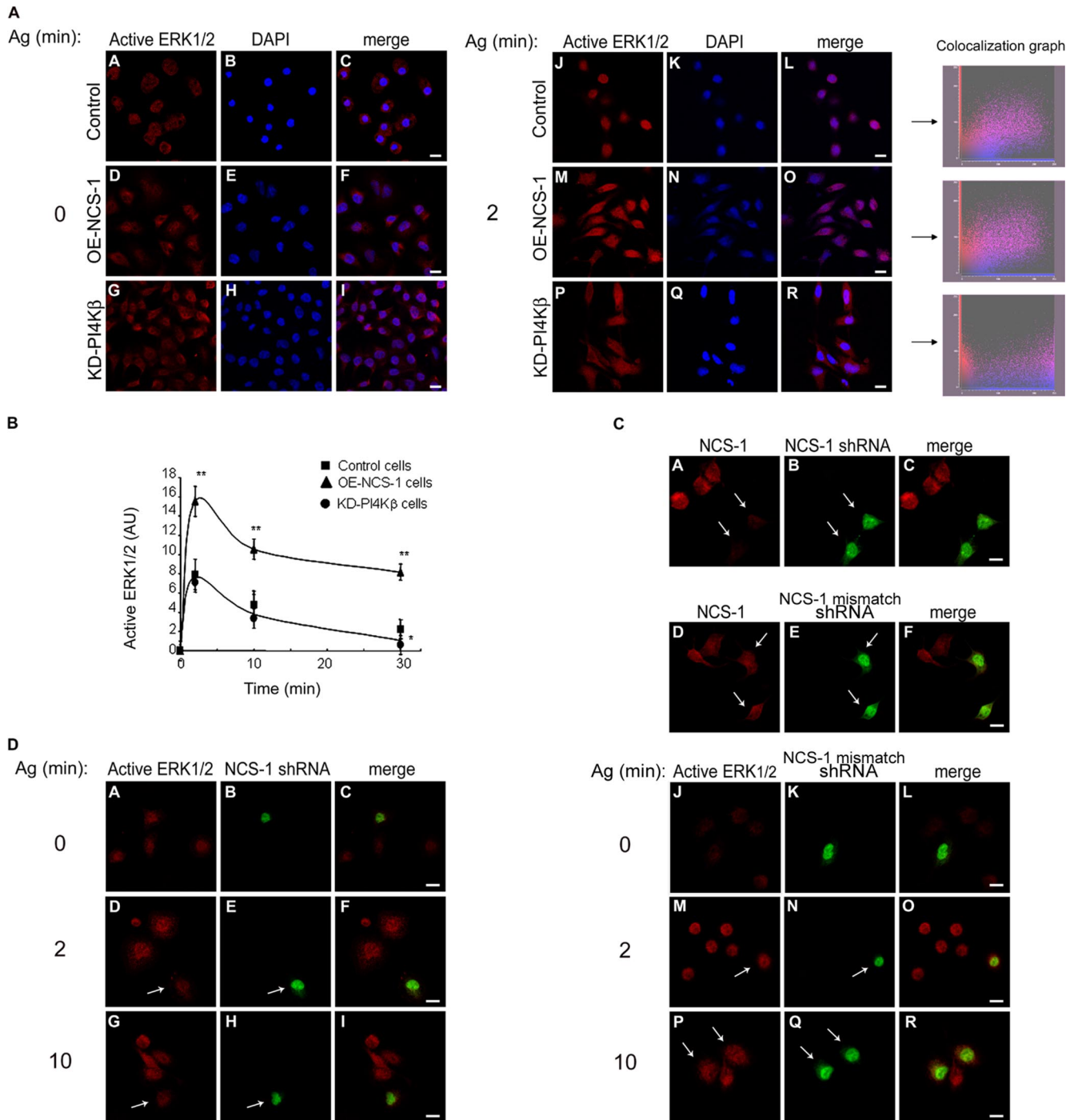
Figure 4. Effect of NCS-1 and KD-PI4Kβ on ERK1/2 phosphorylation and nuclear translocation. (A) IgE-sensitized control (mock-transfected), OE-NCS-1, or KD-PI4Kβ cells were grown on glass coverslips and either left untreated (time 0) or incubated with antigen (Ag, DNP-HAS; 50 ng/ml) for 2 min. Cells were subsequently double stained with monoclonal anti active ERK1/2 antibodies followed by Cy3-conjugated anti-mouse IgG (red) and DAPI for nuclear staining (blue). To compare the extent of nuclear localization of phospho-ERK1/2, the intensity of ERK1/2 immunofluorescence measured was normalized, and double color colocalization analysis was performed for magnified cells. (B) IgE-sensitized control (mock-transfected), OE-NCS-1, or KD-PI4Kβ cells were incubated with antigen (Ag, DNP-HAS; 50 ng/ml) for the indicated times. Cells were subsequently lysed as described under *Materials and Methods*, resolved by SDS-PAGE, subjected to Western blot analysis, and probed with anti-active ERK1/2 antibodies. The intensities of the bands corresponding to pp42 and pp44 (ERK1/2) were quantified by densitometry. The data points presented are means ± SEM of three determinations of three independent experiments. Statistical analysis was performed using one-tailed Mann–Whitney *t* test with *p < 0.05 and **p < 0.01. (C) RBL cells transiently transfected with YFP-NCS-1 shRNA (A–C) or control YFP-NCS-1 mismatched shRNA (D–F) were grown on glass coverslips. Twenty-four hours later, cells were stained with anti NCS-1 antibodies followed by Cy3-conjugated anti-rabbit IgG. Cells were visualized by laser confocal microscopy. The arrows point to transfected cells. Bar, 8 μm. (D) RBL cells transiently transfected with YFP-NCS-1 shRNA (A–I) or control YFP-NCS-1 mismatched shRNA (J–R) were grown on glass coverslips, sensitized with DNP-specific IgE, and activated with DNP-HSA (Ag, 50 ng/ml) for the indicated times. Cells were then stained with monoclonal anti-active ERK1/2 followed by Cy3-conjugated anti-mouse IgG. Cells were visualized by laser confocal microscopy. The arrows point to transfected cells. Bar, 8 μm.
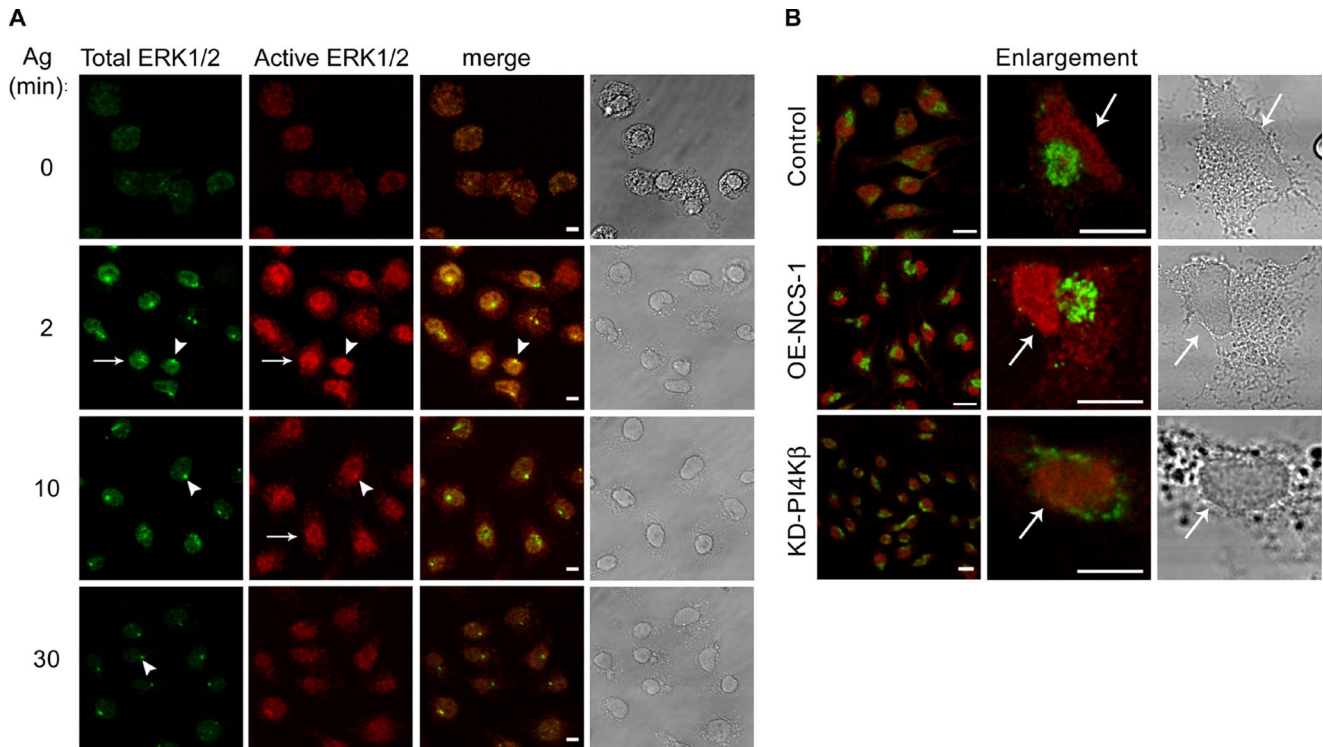
Figure 5. Cellular localization of active and total ERK1/2 in antigen-treated cells. IgE-sensitized RBL (A and B), OE-NCS-1 (B), or KD-PI4Kβ (B) cells were grown on glass coverslips and subsequently either left untreated (time 0) or incubated with antigen (Ag, DNP-HSA, 50 ng/ml) for the indicated times. Cells were then gently permeabilized with 100 μg/ml digitonin as described under *Materials and Methods* and double stained with polyclonal anti ERK1/2 (total ERK1/2) and monoclonal anti active ERK1/2 followed by fluorescein isothiocyanate-conjugated anti rabbit and Cy3-conjugated anti-mouse IgGs. Cells were visualized by laser confocal microscopy. Bars, 8 μm (A) and 10 μm (B). The arrows point to the nucleus (A and B), and arrowheads point to the perinuclear enzymes. Shown on the right are the corresponding phase contrast images.

Presentation of Data

The results presented are representative of at least three similar experiments. Statistical analysis was performed using one-tailed Mann–Whitney *t* test with *p < 0.05 and **p < 0.01.

RESULTS

NCS-1 Decreases, whereas KD-PI4Kβ Increases, the Amount of Internalized Tfn

To investigate whether NCS-1 and PI4Kβ modulate endocytic trafficking, we have compared Tfn uptake by stable RBL cell lines that overexpress either NCS-1 (OE-NCS-1) or a kinase dead mutant of PI4Kβ (KD-PI4Kβ). We have described these cell lines and demonstrated their viability and ability to undergo Ca^{2+}-triggered exocytosis in previous publications (Kapp-Barnea *et al.*, 2003). At time 0, following 1 h of binding at 4°C, all cells displayed comparable amounts of bound Tfn; therefore, indicating that their Tfn-binding capacity was neither affected by NCS-1 nor by the KD mutant of PI4Kβ (Figure 1). However, following 10 min at 37°C, the levels of internalized Tfn were significantly (by ~60%) lower in OE-NCS-1 cells compared with control cells, whereas the KD-PI4Kβ cells contained higher amounts (~3-fold) of Tfn (Figure 1). These results therefore suggested that NCS-1 might either restrain Tfn internalization or enhance its rate of recycling. To distinguish between these possibilities, we have also assessed the effects of NCS-1 and KD-PI4Kβ directly on Tfn recycling. Indeed, examining the levels of Alexa-488-Tfn retained in cells loaded for 1 h before chasing with unlabeled Tfn revealed reduced amounts of Tfn in OE-NCS-1 cells and larger amounts in cells expressing

the KD-PI4Kβ mutant (Figure 2A). Quantitative analysis of the results has indicated a 20% reduction in intracellular Alexa-488-Tfn in control cells chased for 5 min, ~4% reduction in KD-PI4Kβ–expressing cells and 40% in the OE-NCS-1 cells (Figure 2B). In a similar manner, at 20 min after chase, 25% reduction in intracellular Alexa-488-Tfn was recorded in control cells, 12% in KD-PI4Kβ–expressing cells, and 50% reduction in OE-NCS-1 cells (Figure 2B). At longer times (40 min), ~70% of Tfn is recycled from all cells (Figure 2B).

Following the fate of Alexa-488-Tfn in living cells confirmed that at steady state higher amounts of Tfn are detected at the ERC of KD-PI4Kβ–expressing cells compared with OE-NCS-1 cells (Supplemental Movie 1). This analysis also clearly demonstrated that the rate of Tfn export from the ERC was significantly higher in OE-NCS-1 cells compared with KD-PI4Kβ–expressing cells (Supplemental Movie 1). Furthermore, although in OE-NCS-1 cells Alexa-488-Tfn has acquired a clear vectorial movement from the ERC toward the cell surface, in the KD-PI4Kβ–expressing cells, Alexa-488-Tfn randomly moved in and out the ERC (Supplemental Movie 1).

NCS-1 Localizes to the ERC

Previous studies have firmly established that NCS-1 distributes between the *trans*-Golgi network (TGN) and the plasma membrane (Martone *et al.*, 1999; Bourne *et al.*, 2001; O'Callaghan *et al.*, 2002). Indeed, we (Kapp-Barnea *et al.*, 2003) have previously shown that NCS-1 colocalizes with PI4Kβ, whose Golgi localization is well established (De Matteis *et al.*, 2002), at a perinuclear location. However, such perinuclear location might also
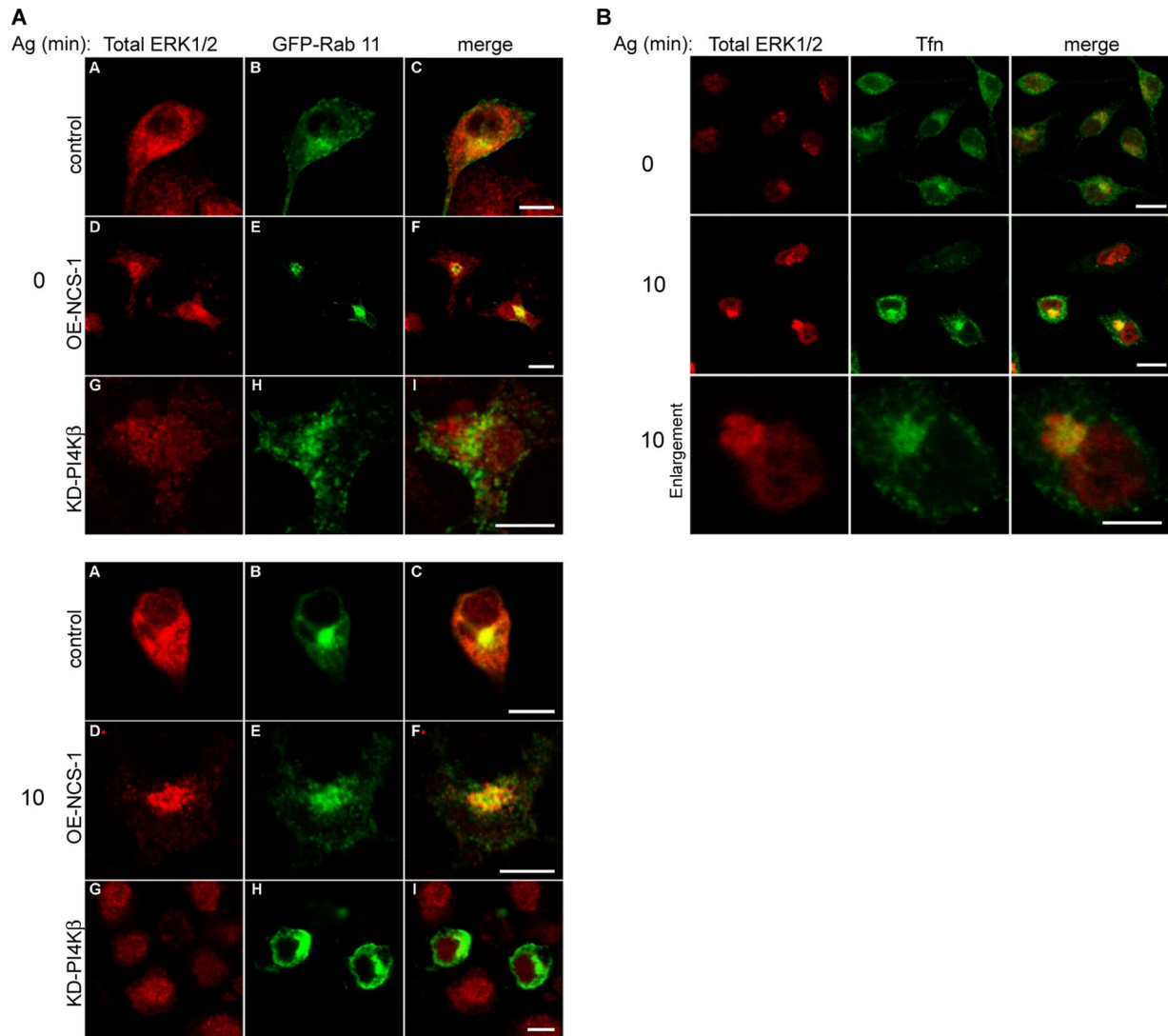
Figure 6. Antigen-induced translocation of ERK1/2 to the ERC. (A) IgE sensitized control (mock-transfected), OE-NCS-1, or KD-PI4Kβ cells were transiently transfected with GFP-Rab 11 cDNA. Cells were subsequently grown on glass coverslips and either left untreated (time 0) or incubated with antigen (Ag, DNP-HSA, 50 ng/ml) for 10 min. Cells were then gently permeabilized with 100 μg/ml digitonin as described under *Materials and Methods* and stained with polyclonal anti ERK1/2 (Total ERK1/2) followed by Cy3-conjugated anti-rabbit IgG. Cells were visualized by laser confocal microscopy. Bar, 10 μm. (B) IgE sensitized control cells were grown on glass coverslips, serum starved for 1 h, and incubated with 50 μg/ml Alexa-488-Tfn for 45 min at 37°C. Cells were subsequently left untreated (time 0) or incubated with antigen (Ag, DNP-HSA, 50 ng/ml) for 10 min. Cells were then gently permeabilized with 100 μg/ml digitonin and stained with polyclonal anti ERK1/2 (total ERK1/2). Bar, 10 μm.

include the ERC, which also resides at the microtubule organizing center (Hopkins and Trowbridge, 1983). Therefore, to address directly this possibility, we investigated NCS-1 localization with regard to ERC-loaded Tfn (Peng *et al.*, 2002; Grimberg *et al.*, 2003; Haberman *et al.*, 2003) and the small GTPase Rab 11 (Ullrich *et al.*, 1996). Indeed, staining of NCS-1 in OE-NCS-1 cells expressing GFP-Rab 11 or monitoring the localization of NCS-1-YFP in cells loaded with TR-conjugated Tfn has demonstrated that a fraction of NCS-1 colocalizes with both Tfn and Rab 11 (Figure 3). These results are therefore conceivable with the notion that a proportion of NCS-1 is present at the ERC.

NCS-1 Stimulates FcεRI-triggered Activation of ERK1/2 MAPKs

Consistent with previous results (Fukamachi *et al.*, 1993; Razin *et al.*, 1995; Turner and Kinet, 1999), exposing IgE-

sensitized cells to the appropriate antigen resulted in the rapid phosphorylation of ERK1/2 (Figure 4, A and B). However, both the extent and the duration of phosphorylation were significantly increased in OE-NCS-1 cells (Figure 4, A and B). To substantiate these results further, we have also examined the effect on ERK1/2 activation of silencing the endogenous NCS-1 by RNA interference. Cells transfected with NCS-1 shRNA, as evident by the expression of YFP, displayed markedly reduced amounts of NCS-1 (Figure 4C). YFP-expressing cells also displayed significantly diminished staining with anti-phospho-ERK antibodies, indicating the existing correlation between the amount of NCS-1 expressed and the extent of ERK1/2 activation (Figure 4D). This effect was specific, because active phospho-ERK1/2 was readily detected in cells transfected with control YFP-shRNA (Figure 4D), which does not affect NCS-1 expression (Figure 4C). Notably, because of the low degree of transfection with the
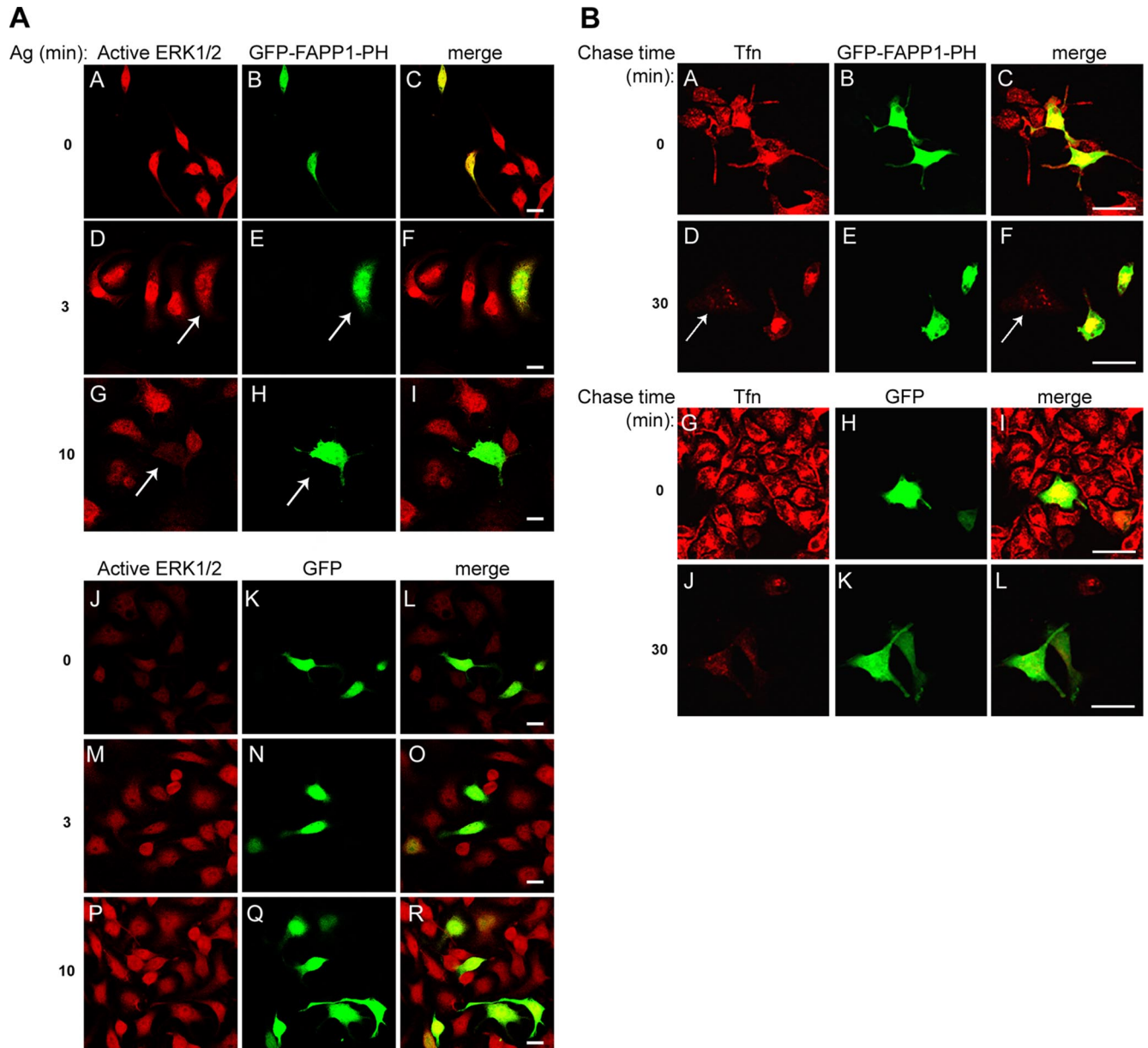
Figure 7. Effect of FAPP1-PH domain on ERK1/2 activation and Tfn recycling. (A) RBL cells transiently transfected with GFP-FAPP1-PH (A–I) or EGFP (J–R) cDNA were grown on glass coverslips, sensitized with DNP-specific IgE, and activated with DNP-HSA (Ag, 50 ng/ml) for the indicated times. Cells were then stained with monoclonal anti-active ERK1/2 followed by Cy3-conjugated anti-mouse IgG. Cells were visualized by laser confocal microscopy. The arrows point to transfected cells. Bar, 20 μm. (B) RBL cells transiently transfected GFP-FAPP1-PH (A–F) or enhanced green fluorescent protein (EGFP) cDNA (G–L) were grown on glass coverslips, serum starved for 1 h, and incubated with 50 μg/ml TR Tfn for 1 h at 37°C. Cells were then placed on ice or washed and chased with 100 μg/ml unlabeled Tfn in the presence of 100 μM defroxamine mesylate for 30 min, as indicated. Cells were visualized by laser confocal microscopy. The arrow points to a nontransfected cell. Bar, 20 μm.

NCS-1 shRNA vector, we could not quantify the extent of NCS-1 knockdown in RBL cells. However, transfection of the highly transfectable human embryonic kidney 293 cells, which express NCS-1 endogenously, with same silencer vector reduced the cellular level of NCS-1 by >70% (our unpublished data).

Attenuation of ERK1/2 activation after antigen stimulation was also observed in cells expressing KD-PI4Kβ (Figure 4B). Strikingly, although a considerable amount of phospho-ERK1/2 could be detected in the nucleus of control and

OE-NCS-1 cells, phospho-ERK1/2 remained mainly cytosolic in KD-PI4Kβ–expressing cells (Figure 4A).

The ERC Is an Intermediate Compartment in the Route of Trafficking of ERK1/2

To investigate whether the effects of NCS-1 and KD-PI4Kβ on ERK1/2 activation and nuclear position were related to their respective stimulatory or inhibitory effects on recycling from the ERC, we investigated the possibility that the ERC was an intermediate station in ERK1/2 trafficking. For this
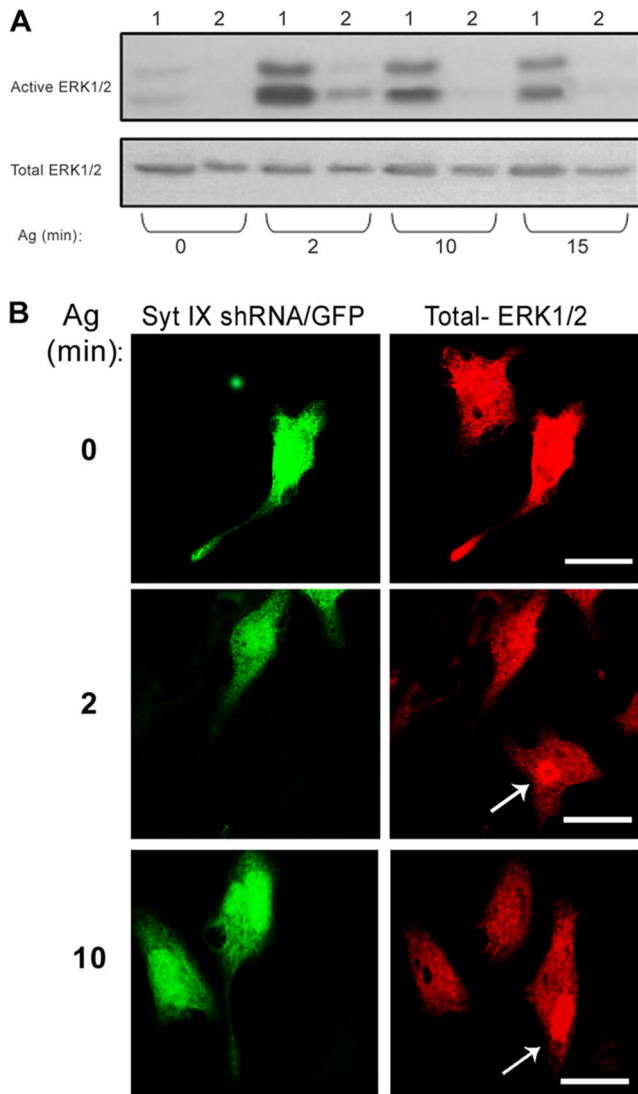
Figure 8. Effect of Syt IX shRNA on ERK1/2 activation and localization. (A) OE-NCS-1 cells, nontransfected (1), or transiently transfected with Syt IX shRNA (2) were sensitized with DNP-specific IgE and activated with DNP-HSA (Ag, 50 ng/ml) for the indicated times. Cell lysates were resolved by SDS-PAGE, subjected to Western blot analysis, and probed with anti-active ERK1/2 antibodies, and reprobed with anti total ERK1/2, as indicated. (B) OE-NCS-1 cells were transiently transfected with Syt IX shRNA and EGFP vector (5:1). Cells were then grown on glass coverslips, sensitized with DNP-specific IgE and, activated with DNP-HSA (Ag, 50 ng/ml) for the indicated times. Cells were subsequently gently permeabilized with 100 μg/ml digitonin and stained with polyclonal anti ERK1/2 (total ERK/2), followed by Cy3-conjugated anti-rabbit IgG, and visualized by laser confocal microscopy. The arrows indicate the position of the ERC in nontransfected cells. Bar, 10 μm.

purpose, cells were permeabilized with digitonin to allow leakage of the cytosol. This procedure enables better detection of proteins that are distributed between the cytosol and intracellular organelles, such as the Golgi (Wong *et al.*, 1999). As expected, staining of resting cells with anti-ERK1/2 antibodies revealed a weak and diffused staining corresponding to the residual cytosolic kinases (Figure 5A). However, with increasing times of antigen stimulation, the intensity of labeling with anti-total ERK1/2 antibodies increased consistent with the notion that a larger fraction of ERK1/2 became

resistant to leakage from the digitonin-permeabilized cells. Moreover, this increased labeling was linked with partition of the enzymes between the nucleus, where they colocalized with the active kinases stained with anti-active ERK1/2 (Figure 5A, arrows) and a prominent perinuclear region (Figure 5A, arrowheads). Notably, although most of the active kinases localized to the nucleus, careful analysis revealed their presence also at the perinuclear site (Figure 5A, arrowheads). With increasing time after triggering, staining with anti-active ERK1/2 antibodies decayed, reflecting the dephosphorylation of the kinases, but nonactive kinases could still be detected at the perinuclear site (Figure 5A, arrowheads). This pattern was particularly evident in antigen-triggered OE-NCS-1 cells (Figure 5B). In sharp contrast, the enzymes remained mostly cytosolic in KD-PI4Kβ cells (Figure 5B). Thus, a close correlation exists between the amount of ERC-localized ERK1/2 and the amount of nucleus-localized active kinases, whereby overexpression of NCS-1 has increased the amount of both ERC localized ERK1/2 and nuclear phospho-ERK1/2, whereas KD-PI4Kβ decreased both.

That the perinuclear localization of ERK1/2 corresponded to the ERC was indicated by their colocalization with both Rab 11- and ERC-localized Tfn (Figure 6, A and B). Notably, the distribution of Rab 11 seemed somewhat different in the KD-PI4Kβ cells, in which the protein seemed more diffused and a fraction of it localized to the plasma membrane (Figure 6A). However, because both PI4Kβ and its KD mutant bind with equal potency Rab 11 (de Graaf, 2004), it is not surprising that overexpression of KD-PI4Kβ influences the localization of Rab 11.

FAPP1-PH Domain Inhibits Activation and Nuclear Localization of ERK1/2 as Well as Export of Tfn from the ERC

The findings that NCS-1 stimulates and KD-PI4Kβ inhibits recycling and nuclear transport of ERK1/2 suggested that PI4Kβ may mediate NCS-1 function. To investigate this possibility directly, we examined whether the PH domain of FAPP1, a PI(4)P binding protein (Levine and Munro, 2002; Godi *et al.*, 2004), could impede ERK1/2 activation and nuclear translocation. Indeed, staining of cells transiently transfected with GFP-FAPP1-PH with anti-phospho-ERK1/2 revealed a profound reduction in the amount of active ERK1/2 in GFP-FAPP1-PH–expressing cells (Figure 7A). In contrast, introduction of soluble GFP, as a control, had no effect (Figure 7A).

To further establish the link between PI(4)P and recycling through the ERC, we also examined the effect of FAPP1-PH on Tfn recycling. Indeed, in cells expressing GFP-FAPP1-PH, export of ERC-localized Tfn was clearly inhibited (Figure 7B). Thus, after 30 min of chase, Tfn could only be detected in GFP-FAPP1-PH–transfected cells (Figure 7, B and D–F), whereas in nontransfected cells or in cells transfected with free cytosolic GFP (Figure 7B and J–L), Tfn was barely detected.

Inhibition of Recycling Abrogates Activation of ERK1/2

Previously, we showed that Syt IX is required for export of Tfn from the ERC to the cell surface (Haberman *et al.*, 2003). Therefore, to investigate whether export from the ERC was required for the maintenance of ERK1/2 in an active state, we used shRNA to knockdown Syt IX. Consistent with the implied role of recycling from the ERC in ERK activation, Syt IX shRNA dramatically inhibited FcεRI-induced activation of ERK1/2 (Figure 8A) as well as positioning of the kinases at the ERC (Figure 8B).
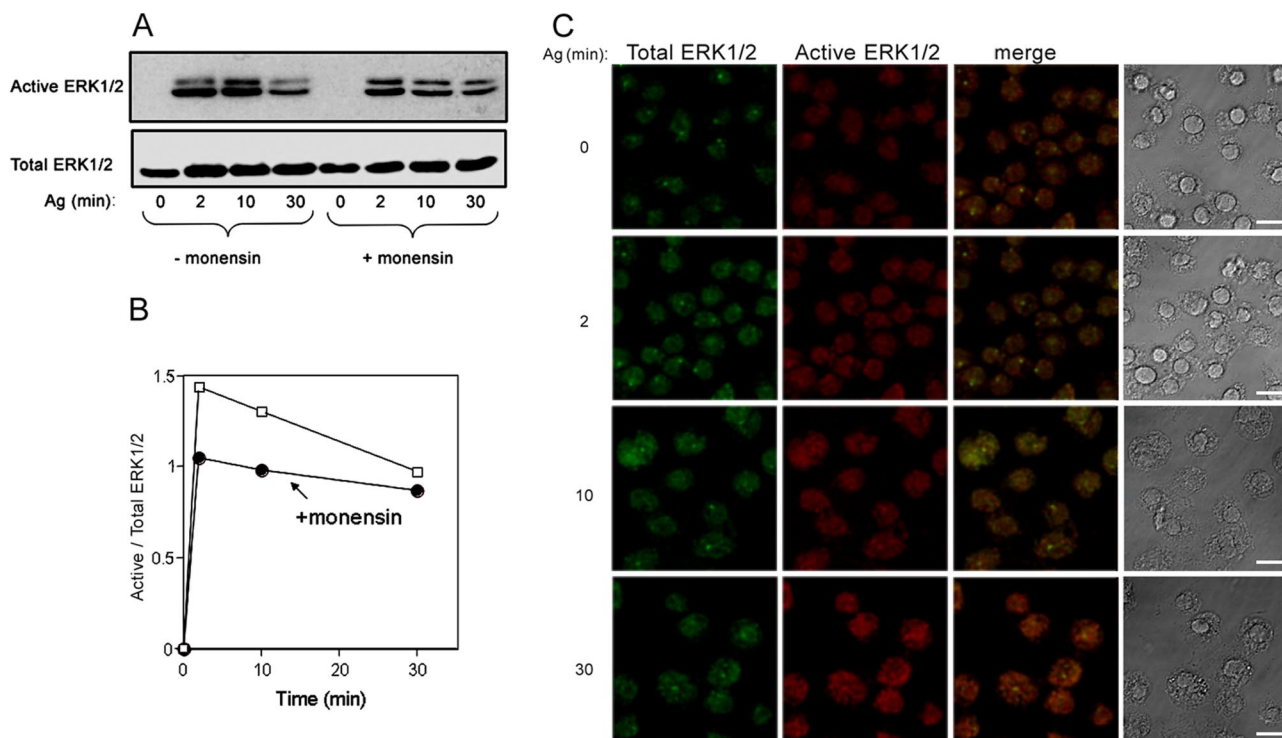
Figure 9. Effect of monensin on ERK1/2 activation and localization. (A) IgE-sensitized RBL cells were either left untreated or treated with 1 μM monensin for 2 h before activation with DNP-HSA (Ag, 50 ng/ml) for the indicated times. Cells were subsequently lysed, and cell lysates were resolved by SDS-PAGE and immunoblotted with anti-active ERK1/2. Blots were then reprobed with antibodies directed against ERK1/2 (total ERK1/2). (B) Densitometric analysis of the results presented in A. (C) IgE sensitized RBL cells were treated with 1 μM monensin for 2 h, washed, and incubated with DNP-HSA (Ag, 50 ng/ml) for the indicated times. Cells were analyzed as described under Figure 5A. Bar, 8 μm.

To corroborate these results further, we also explored the effect of monensin, which is known to inhibit recycling (Carpentier *et al.*, 1984; Stein *et al.*, 1984), on ERK1/2 activation. Indeed, this set of experiments has clearly demonstrated that in FcεRI-stimulated, but monensin-treated RBL cells, although ERK1/2 were activated and only moderately inhibited by monensin, as indicated by immunoblotting with anti-active-ERK1/2 (Figure 9, A and B), their translocation to the nucleus was completely prevented, resulting in a significantly lower immunofluorescence signal when staining digitonin-permeabilized cells (Figure 9C compared with 5A). Consistent with the observed correlation between the amount of nuclear active ERK1/2 and the amount of ERC associated inactive ERK1/2, considerably less ERK1/2 was retained in perinuclear structures in monensin-treated cells (Figure 9C).

Neither NCS-1 nor KD-PI4Kβ Affects Akt/PKB Activation

Activation of the FcεRI in RBL cells results in the activation of phosphoinositide-3 kinase (PI3K) (Laffargue *et al.*, 2002). Subsequent phosphorylation of phosphatidylinositol(3) phosphate to form phosphatidylinositol 3,4,5-trisphosphate then leads to the concomitant activation of Akt/protein kinase B (PKB) (Djouder *et al.*, 2001). Therefore, we investigated whether NCS-1 and KD-PIKβ also contribute to the PI3K signaling output. For this purpose, we have monitored the phosphorylation state of Akt/PKB upon antigen triggering. Indeed, Western blot analysis using antibodies directed against the phosphorylated form of Akt (Ser 473) revealed the presence of phospho-Akt already at 5 min postantigen trigger and the enzyme remained phosphorylated also at 15

min (Figure 10). However, no significant differences were detected between control, OE-NCS-1 or KD-PI4Kβ cells (Figure 10), indicating that this signaling network is unaffected by NCS-1 or PI4Kβ.

NCS-1 Stimulates and KD-PI4Kβ Inhibits Release of AA Metabolites

In mast cells, activation of ERK1/2 results in the release of metabolites of AA, thereby contributing to the propagation of the late-phase inflammation associated with the allergic reaction (Zhang et al., 1997). Therefore, to investigate the physiological relevance of the regulatory functions of NCS-1 and PI4Kβ, we investigated their ability to modulate FcεRI-triggered release of AA metabolites. Indeed, these experiments demonstrated that NCS-1 significantly potentiates (by 3-fold), whereas KD-PI4Kβ inhibits (by 6-fold) FcεRI-trig-
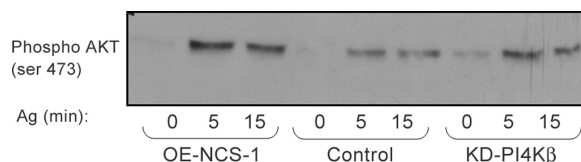

Figure 10. Effect of NCS-1 or KD-PI4Kβ on Akt/PKB phosphorylation. Control, OE-NCS-1, or KD-PI4Kβ cells were IgE-sensitized and activated by DNP-HSA (Ag, 50 ng/ml) for the indicated times. Cells were subsequently lysed, and cell lysates were resolved by SDS-PAGE and immunoblotted with anti-phospho (Ser 473)-Akt antibodies.
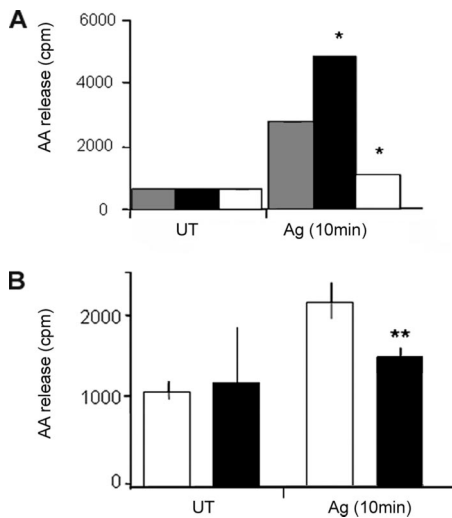
Figure 11. Effect of NCS-1 and KD-PI4Kβ on AA/metabolites release. (A) IgE-sensitized control (mock-transfected, shaded columns), OE-NCS-1 (filled columns), or KD-PI4Kβ cells (open columns) were loaded with [³H]AA. Buffer (UT) or DNP-HSA (Ag, 50 ng/ml) was subsequently added, and the cells incubated for further 10 min. AA release was then determined as described under *Materials and Methods*. (B) RBL cells were transiently transfected with GFP-FAPP1-PH (filled columns) or with an empty EGFP vector (open columns). Transfected cells were then sorted and collected by FACS and loaded with [³H]AA as described under *Materials and Methods*. Cells were subsequently sensitized with DNP specific IgE and incubated for 10 min with either buffer (UT) or DNP-HSA (Ag, 50 ng/ml). AA release was determined as described under *Materials and Methods*. The data points presented are means ± SEM of three determinations of three independent experiments. Statistical analysis was performed using one-tailed Mann–Whitney *t* test with *p < 0.05 and **p <0.01.

gered release of AA/metabolites (Figure 11A). To gain further support to this notion, we have also compared AA/metabolites release of control cells with that of GFP-FAPP1-PH–expressing cells, which we sorted and collected by a fluorescence-activated cell sorter (FACS). These experiments confirmed that introduction of the FAPP1-PH domain significantly (>60%) reduced FcεRI-triggered release of AA/metabolites (Figure 11B), confirming the requirement of PI(4)P for this process.

DISCUSSION

PI4Kβ is a downstream target for NCS-1 in a number of exocytic processes, including control of regulated secretion in both neuroendocrine (Rajebhosale *et al.*, 2003) and nonneuronal cells (Kapp-Barnea *et al.*, 2003; Gromada *et al.*, 2005) and regulation of biosynthetic transport (Zhao *et al.*, 2001). Increasing the pool of PI(4,5)P₂ available for PLC-induced hydrolysis and the consequent increase in second messengers generation provide the molecular mechanism by which NCS-1 stimulates exocytosis. However, in view of the major roles played by phosphoinositides in controlling endocytic pathways, both by defining specific functional domains along endocytic organelles and by modulating membrane or protein–protein interactions (Katan and Allen, 1999; Cockcroft and De Matteis, 2001; De Matteis *et al.*, 2002; Gruenberg, 2003; Itoh and Takenawa, 2004), it is reasonable to postulate that NCS-1 may also participate in controlling endocytic processes. Specifically, in this work, we evaluated

the possible role and mechanism of action of NCS-1 in controlling endocytic processes as well as ERK1/2 signaling, which is known to be tightly linked with endocytosis (Kholodenko, 2002). However, overexpression of neither NCS-1 or a kinase dead mutant of PI4Kβ has manifested any effect on endocytosis as monitored by following the internalization of Tfn. These data therefore exclude PI4Kβ-derived PI(4)P from playing a direct role in plasma membrane to endosome trafficking or contributing to the pool of plasma membrane PI(4,5)P₂, which regulates endocytosis by modulating adaptor or accessory proteins function (Gaidarov and Keen, 2005). Consistent with this notion are the findings that PI(4)P is mainly involved in the recruitment of the adaptor proteins AP-1 and epsinR (Hirst *et al.*, 2003; Mills *et al.*, 2003; Wang *et al.*, 2003), none of which is implicated in internalization from the plasma membrane. In sharp contrast, we found a profound effect of NCS-1 and KD-PI4Kβ on the export of Tfn from the ERC, a distinct recycling compartment that is clustered around the centrosome (Hopkins and Trowbridge, 1983) and that is involved in both receptor and lipid recycling (Nichols *et al.*, 2001) as well as retrograde transport of a number of endogenous proteins, such as TGN38 (Ghosh *et al.*, 1998), and toxins, such as the Shiga toxin (Mallard *et al.*, 1998). PI4Kβ was previously shown to reside at the Golgi (Cockcroft and De Matteis, 2001; De Matteis *et al.*, 2002) and to be essential for TGN-to-plasma membrane transport (Godi *et al.*, 2004). Our data now implicate PI4Kβ and PI(4)P as pivotal components for transport from the ERC to the cell surface. Accordingly, we now show that a fraction of NCS-1 resides at the ERC.

Previous studies have documented the essentiality of endocytic trafficking for ERK1/2 activation and signaling (Gruenberg, 2003; Itoh and Takenawa, 2004). Although active ERK1/2 translocate to the nucleus (Volmat and Pouyssegur, 2001), mathematical calculations based on diffusion coefficients have anticipated that the rate of nuclear import of the activated ERKs could not be simply explained by diffusion of the cytosolic kinases (Kholodenko, 2003). Association with and movement along the endocytic pathway have therefore been suggested as a reasonable solution for the spatial segregation of the activated ERKs and facilitation of their transport toward the nucleus. In line with this notion, our studies mark the pericentriolar ERC as a critical station in ERK signaling. First, we show that during cell triggering, a fraction of ERK1/2 localizes to the ERC, where the enzymes colocalize with Rab 11 and internalized Tfn. We further show that a close correlation exists between the amount of ERC localized ERK1/2 and the amount of nuclear located active phosphokinases. Second, we show that overexpression of NCS-1, which stimulates recycling from the ERC, increases the extent of ERK activation, whereas knockdown of endogenous NCS-1 or expression of KD-PI4Kβ that inhibits recycling diminishes the amount of nucleus-localized active ERKs. Finally, we show that knockdown of Syt IX, a member of the Syt family of proteins, which is required for recycling from the ERC (Haberman *et al.*, 2003), or exposure to monensin, a drug that inhibits recycling (Carpentier *et al.*, 1984; Stein *et al.*, 1984), hampers ERK1/2 activation and in particular abrogates nuclear translocation of the kinases. Therefore, collectively our results implicate PI(4)P as a crucial factor in recycling from the ERC and the ERC as an essential intermediate in activation and nuclear location of ERK1/2. Indeed, introduction of the PI(4)P-binding PH domain of FAPP1, which functions as a scavenger of PI(4)P (Godi *et al.*, 2004), inhibits recycling as well as ERK1/2 activation. This finding joins recent data demonstrating the presence of HRas in the ERC (Gomez and Daniotti, 2005).

Together, these results support the existence of a functional link between recycling through the ERC and the propagation of signaling cascades. Thus, the right balance between input signaling events evolving at the plasma membrane and retrieval of intracellular cargo proteins, including receptors and signaling molecules via active shuttling of the recycling endosome, seems to play a crucial role in maintaining signaling homeostasis. Consistent with this notion is the finding that hypoxia promotes Rab 11-induced trafficking, and this is directly linked to increased invasiveness of tumors (Yoon *et al.*, 2005). Thus, the ERC may serve as a scaffold for the docking of signaling complexes to facilitate their fast retrieval to the plasma membrane to allow additional cycles of signaling. In this context, it is noteworthy that the MAPKs' signal output is higher when the kinases are activated at the plasma membrane rather than in the cytosol (Harding *et al.*, 2005). Therefore, association of the kinases with the ERC should facilitate their positioning at the plasma membrane and thereby serve to amplify their signaling output.

The physiological relevance of this pathway is demonstrated by the observation that NCS-1 stimulates but KD-PI4Kβ inhibits FcεRI-induced release of AA/metabolites, a downstream process from ERK activation in mast cells (Zhang *et al.*, 1997). Moreover, depletion of PI(4)P by introduction of the FAPP1-PH domain inhibits this release, identifying NCS-1 and PI4Kβ as heretofore unrecognized participants in the propagation of inflammatory reactions. Interestingly, in mast cells the effect of NCS-1 is linked specifically to ERK1/2 signaling output, whereas the PI3K limb of FcεRI signaling remains unaffected. In contrast, NCS-1 has recently been implicated as a survival factor in injured neurons by stimulating the PI3K–Akt pathway (Nakamura *et al.*, 2006). Therefore, NCS-1 seems to play a major role in the control of cell growth and survival. Moreover, NCS-1 function might be cell type specific and dependent on its subcellular localization. Thus, plasma membrane localized NCS-1 (e.g., in neurons) may modulate phosphatidylinositol trisphosphate levels and in turn Akt signaling, whereas ERC-localized NCS-1 (e.g., mast cells) may control recycling and in turn ERK1/2 signaling.

ACKNOWLEDGMENTS

REFERENCES

Birkeland, H. C., and Stenmark, H. (2004). Protein targeting to endosomes and phagosomes via FYVE and PX domains. Curr. Top. Microbiol. Immunol. *282*, 89–115.

Bourne, Y., Dannenberg, J., Pollmann, V., Marchot, P., and Pongs, O. (2001). Immunocytochemical localization and crystal structure of human frequenin (neuronal calcium sensor 1). J. Biol. Chem. *276*, 11949–11955.

Braunewell, K. H., and Gundelfinger, E. D. (1999). Intracellular neuronal calcium sensor proteins: a family of EF-hand calcium-binding proteins in search of a function. Cell Tissue Res. *295*, 1–12.

Burgoyne, R. D., and Weiss, J. L. (2001). The neuronal calcium sensor family of Ca^{2+}-binding proteins. Biochem. J. *353*, 1–12.

Carpentier, J. L., Dayer, J. M., Lang, U., Silverman, R., Orci, L., and Gorden, P. (1984). Down-regulation and recycling of insulin receptors. Effect of monensin on IM-9 lymphocytes and U-937 monocyte-like cells. J. Biol. Chem. *259*, 14190–14195.

Chen, C., Yu, L., Zhang, P., Jiang, J., Zhang, Y., Chen, X., Wu, Q., Wu, Q., and Zhao, S. (2002). Human neuronal calcium sensor-1 shows the highest expression level in cerebral cortex. Neurosci. Lett. *319*, 67–70.

Cockcroft, S., and De Matteis, M. A. (2001). Inositol lipids as spatial regulators of membrane traffic. J. Membr. Biol. *180*, 187–194.

De Camilli, P., Emr, S. D., McPherson, P. S., and Novick, P. (1996). Phosphoinositides as regulators in membrane traffic. Science *271*, 1533–1539.

de Graaf, P. (2004). Phosphatidylinositol 4-kinase beta is critical for functional association of rab11 with the Golgi complex. Mol. Biol. Cell *15*, 2038–2047.

De Matteis, M. A., Godi, A., and Corda, D. (2002). Phosphoinositides and the Golgi complex. Curr. Opin. Cell Biol. *14*, 434–447.

Di Fiore, P. P., and De Camilli, P. (2001). Endocytosis and signaling. An inseparable partnership. Cell *106*, 1–4.

Djouder, N., Schmidt, G., Frings, M., Cavalie, A., Thelen, M., and Aktories, K. (2001). Rac and phosphatidylinositol 3-kinase regulate the protein kinase B in FcεRI signaling in RBL 2H3 mast cells. J. Immunol. *166*, 1627–1634.

Fukamachi, H., Takei, M., and Kawakami, T. (1993). Activation of multiple protein kinases including a MAP kinase upon Fc epsilon RI cross-linking. Int. Arch. Allergy Immunol. *102*, 15–25.

Fukuda, M. (2004). RNA interference-mediated silencing of synaptotagmin IX, but not synaptotagmin I, inhibits dense-core vesicle exocytosis in PC12 cells. Biochem. J. *380*, 875–879.

Gaidarov, I., and Keen, J. H. (2005). Membrane targeting of endocytic adaptors: cargo and lipid do it together. Dev. Cell *8*, 801–802.

Godi, A., Di Campli, A., Konstantakopoulos, A., Di Tullio, G., Alessi, D. R., Kular, G. S, Daniele, T., Marra, P., Lucocq, J. M., and De Matteis, M. A. (2004). FAPPs control Golgi-to-cell-surface membrane traffic by binding to ARF and PtdIns(4)P. Nat. Cell Biol. *6*, 393–404.

Gomez, G. A., and Daniotti, J. L. (2005). H-Ras dynamically interacts with recycling endosomes in CHO-K1 cells. Involvement of Rab5 and Rab11 in the trafficking of H-RAS to this pericentriolar endocytic compartment. J. Biol. Chem. *280*, 34997–35010.

Ghosh, R. N., Mallet, W. G., Soe, T. T., McGraw, T. E., and Maxfield, F. R. (1998). An endocytosed TGN38 chimeric protein is delivered to the TGN after trafficking through the endocytic recycling compartment in CHO cells. J. Cell Biol. *142*, 923–936.

Grimberg, E., Peng, Z., Hammel, I., and Sagi-Eisenberg, R. (2003). Synaptotagmin III is a critical factor for the formation of the perinuclear endocytic recycling compartment and determination of secretory granules size. J. Cell Sci. *116*, 145–154.

Gromada J., *et al.* (2005). Neuronal calcium sensor-1 potentiates glucose-dependent exocytosis in pancreatic beta cells through activation of phosphatidylinositol 4-kinase beta. Proc. Natl. Acad. Sci. USA *102*, 10303–10308.

Gruenberg, J. (2003) Lipids in endocytic membrane transport and sorting. Curr. Opin. Cell Biol. *15*, 382–388.

Haberman, Y., Grimberg, E., Fukuda, M., and Sagi-Eisenberg, R. (2003). Synaptotagmin IX, a possible linker between the perinuclear endocytic recycling compartment and the microtubules. J. Cell Sci. *116*, 4307–4318.

Harding, A., Tian, T., Westbury, E., Frische, E., and Hancock, J. F. (2005). Subcellular localization determines MAP kinase signal output. Curr. Biol. *15*, 869–873.

Haynes, L. P., Thomas, G. M., and Burgoyne, R. D. (2005). Interaction of neuronal calcium sensor-1 and ADP-ribosylation factor 1 allows bidirectional control of phosphatidylinositol 4-kinase beta and trans-Golgi network-plasma membrane traffic. J. Biol. Chem. *280*, 6047–6054.

Hendricks, K. B., Wang, B. Q., Schieders, E. A., and Thorner, J. (1999). Yeast homologue of neuronal frequenin is a regulator of phosphatidylinositol-4-OH kinase. Nat. Cell Biol. *1*, 234–241.

Hirst, J., Motley, A., Harasaki, K., Peak, Chew, S. Y., and Robinson, M. S. (2003). EpsinR: an ENTH domain-containing protein that interacts with AP-1. Mol. Biol. Cell *14*, 625–641.

Hopkins, C. R., and Trowbridge, I. S. (1983). Internalization and processing of transferrin and the transferrin receptor in human carcinoma A431 cells. J. Cell Biol. *97*, 508–521.

Hurley, J. H., and Meyer, T. (2001). Subcellular targeting by membrane lipids. Curr. Opin. Cell Biol. *13*, 146–152.

Itoh, T., and Takenawa, T. (1993). Regulation of endocytosis by phosphatidylinositol 4,5-bisphosphate and ENTH proteins. Curr. Top. Microbiol. Immunol. *282*, 31–47.

Itoh, T., and Takenawa, T. (2002). Phosphoinositide-binding domains: functional units for temporal and spatial regulation of intracellular signalling. Cell. Signal. *14*, 733–743.

Jeromin, A., Shayan, A., Msghine, M., Roder, J., and Atwood, H. (1999). Crustacean frequenins: molecular cloning and differential localization at neuromuscular junctions. J. Neurobiol. *41*, 165–175.

Kapp-Barnea, Y., Melnikov, S., Shefler, I., Jeromin, A., and Sagi-Eisenberg, R. (2003). Neuronal calcium sensor-1 and phosphatidylinositol 4-kinase beta regulate IgE receptor-triggered exocytosis in cultured mast cells. J. Immunol. *171*, 5320–5327.

Katan, M., and Allen, V. L. (1999). Modular PH and C2 domains in membrane attachment and other functions. FEBS Lett. *452*, 36–40.

Kholodenko, B. N. (2002). MAP kinase cascade signaling and endocytic trafficking: a marriage of convenience? Trends Cell Biol. *206*, 173–177.

Kholodenko, B. N. (2003). Four-dimensional organization of protein kinase signaling cascades: the roles of diffusion, endocytosis and molecular motors. J. Exp. Biol. *206*, 2073–2082.

Laffargue, M., Calvez, R., Finan, P., Trifilieff, A., Barbier, M., Altruda, F., Hirsch, E., and Wymann, M. P. (2002). Phosphoinositide 3-kinase gamma is an essential amplifier of mast cell function. Immunity *16*, 441–451.

Levine, T. P., and Munro, S. (2002). Targeting of Golgi-specific pleckstrin homology domains involves both PtdIns 4-kinase-dependent and -independent components. Curr. Biol. *12*, 695–704.

Lunin, V. V., Munger, C., Wagner, J., Ye, Z., Cygler, M., and Sacher, M. (2004). The structure of the MAPK scaffold, MP1, bound to its partner, p14. A complex with a critical role in endosomal map kinase signaling. J. Biol. Chem. *279*, 23422–23430.

Mallard, F., Antony, C., Tenza, D., Salamero, J., Goud, B., and Johannes, L. (1998). Direct pathway from early/recycling endosomes to the Golgi apparatus revealed through the study of shiga toxin B-fragment transport. J. Cell Biol. *143*, 973–990.

Martone, M. E., Edelmann, V. M., Ellisman, M. H., and Nef, P. (1999). Cellular and subcellular distribution of the calcium-binding protein NCS-1 in the central nervous system of the rat. Cell Tissue Res. *295*, 395–407.

McFerran, B., Graham, M., and Burgoyne, R. (1998). Neuronal Ca^{2+} Sensor 1, the mammalian homologue of frequenin, is expressed in Chromaffin and PC12 cells and regulates neurosecretion from dense-core granules. J. Biol. Chem. *273*, 22768–22772.

Miaczynska, M., Pelkmans, L., and Zerial, M. (2004). Not just a sink: endosomes in control of signal transduction. Curr. Opin. Cell Biol. *16*, 400–406.

Mills, I. G., Praefcke, G. J., Vallis, Y., Peter, B. J., Olesen, L. E., Gallop, J. L., Butler, P. J., Evans, P. R., and McMahon, H. T. (2003). EpsinR: an AP1/clathrin interacting protein involved in vesicle trafficking. J. Cell Biol. *160*, 213–222.

Nakamura, T. Y., Jeromin, A., Smith, G., Kurushima, H., Koga, H., Nakabeppu, Y., Wakabayashi, S., and Nabekura, J. (2006). Novel role of neuronal Ca2+ sensor-1 as a survival factor up-regulated in injured neurons. J. Cell Biol. *172*, 1081–1091.

Nichols, B. J., Kenworthy, A. K., Polishchuk, R. S., Lodge, R., Roberts, T. H., Hirschberg, K., Phair, R. D., and Lippincott-Schwartz, J. (2001). Rapid cycling of lipid raft markers between the cell surface and Golgi complex. J. Cell Biol. *153*, 529–541.

O'Callaghan, D. W., Ivings, L., Weiss, J. L., Ashby, M. C., Tepikin, A. V., and Burgoyne, R. D. (2002). Differential use of myristoyl groups on neuronal calcium sensor proteins as a determinant of spatio-temporal aspects of Ca^{2+} signal transduction. J. Biol. Chem. *277*, 14227–14237.

Peng, Z., Grimberg, E., and Sagi-Eisenberg, R. (2002). Suppression of Synaptotagmin II restrains phorbolester-induced downregulation of protein kinase Calpha by diverting the kinase from a degradative pathway to the recycling endocytic compartment. J. Cell. Sci. *115*, 3083–3092.

Pouyssegur, J., Volmat, V., and Lenormand, P. (2002). Fidelity and spatio-temporal control in MAP kinase (ERKs) signalling. Biochem. Pharmacol. *64*, 755–763.

Rajebhosale, M., Greenwood, S., Vidugiriene, J., Jeromin, A., and Hilfiker, S. (2003). Phosphatidylinositol 4-OH kinase is a downstream target of neuronal calcium sensor-1 in enhancing exocytosis in neuroendocrine cells. J. Biol. Chem. *278*, 6075–6084.

Razin, E., Pecht, I., and Rivera, J. (1995). Signal transduction in the activation of mast cells and basophils. Immunol. Today *16*, 370–373.

Roth, M. G. (2004). Phosphoinositides in constitutive membrane traffic. Physiol. Rev. *84*, 699–730.

Seger, R., and Krebs, E. G. (1995). The MAPK signaling cascade. FASEB J. *9*, 726–735.

Sippy, T., Cruz-Martin, A., Jeromin, A., and Schweizer, F. E. (2003). Acute changes in short-term plasticity at synapses with elevated levels of neuronal calcium sensor-1. Nat. Neurosci. *6*, 1031–1038.

Stein, B. S., Bensch, K. G., and Sussman, H. H. (1984). Complete inhibition of transferrin recycling by monensin in K562 cells. J. Biol. Chem. *259*, 14762–14772.

Turner, H., and Kinet, J. P. (1999). Signalling through the high-affinity IgE receptor Fc epsilonRI. Nature *402*, B24–B30.

Volmat, V., and Pouyssegur, J. (2001). Spatiotemporal regulation of the p42/p44 MAPK pathway. Biol. Cell *93*, 71–79.

Ullrich, O., Reinsch, S., Urbe, S., Zerial, M., and Parton, R. G. (1996). Rab11 regulates recycling through the pericentriolar recycling endosome. J. Cell Biol. *135*, 913–924.

Wang, Y. J., Wang, J., Sun, H. Q., Martinez, M., Sun, Y. X., Macia, E., Kirchhausen, T., Albanesi, J. P., Roth, M. G., and Yin, H. L. (2003). Phosphatidylinositol 4 phosphate regulates targeting of clathrin adaptor AP-1 complexes to the Golgi. Cell *114*, 299–310.

Wong, S. H., Xu, Y., Zhang, T., Griffiths, G., Lowe, S. L., Subramaniam, V. N., Seow, K. T., and Hong, W. (1999). GS32, a novel Golgi SNARE of 32 kDa, interacts preferentially with syntaxin 6. Mol. Biol. Cell *10*, 119–134.

Yoon, S. O., Shin, S., and Mercurio, A. M. (2005). Hypoxia stimulates carcinoma invasion by stabilizing microtubules and promoting the Rab11 trafficking of the alpha6beta4 integrin. Cancer Res. *65*, 2761–2769.

Zhang, C., Baumgartner, R. A., Yamada, K., and Beaven, M. A. (1997). Mitogen-activated protein (MAP) kinase regulates production of tumor necrosis factor-alpha and release of arachidonic acid in mast cells. Indications of communication between p38 and p42 MAP kinases. J. Biol. Chem. *272*, 13397–13402.

Zhao, X., Varnai, P., Tuymetova, G., Balla, A., Toth, Z. E., Oker-Blom, C., Roder, J., Jeromin, A., and Balla, T. (2001). Interaction of neuronal calcium sensor-1 (NCS-1) with phosphatidylinositol 4-kinase beta stimulates lipid kinase activity and affects membrane trafficking in COS-7 cells. J. Biol. Chem. *276*, 40183–40189.